

THE STATISTICAL EVALUATIONS OF TRANSMISSION CHARACTERISTICS, LIMITS OF RANGES AND SPEEDS OF TRANSMISSION OF INFORMATION VIA THE PULSED ATMOSPHERIC BISTATIC OPTICAL CHANNELS

Mikhail V. Tarasenkov¹, Egor S. Poznakharev² and Vladimir V. Belov¹

¹ *V.E. Zuev Institute of atmospheric optics, SB of RAS, Tomsk, Russia*

² *Tomsk state University, Tomsk, Russia*

E-mail: belov@iao.ru; tmv@iao.ru

ABSTRACT

The simulation program by the Monte Carlo method of pulse reactions of bistatic atmospheric aerosol-gas channels of optical-electronic communication systems (OECS) is created on the basis of the modified double local estimation algorithm. It is used in a series of numerical experiments in order to evaluate statistically the transfer characteristics of these channels depending on the optical characteristics of an atmosphere plane-parallel model for wavelengths $\lambda = 0.3, 0.5,$ and $0.9 \mu\text{m}$ at a meteorological visibility range $S_M = 10$ and 50 km. The results are obtained for a set of basic distances between the light source and the light receiver up to 50 km and for the angular orientations of the optical axes of a laser radiation beam and of the receiving system in a wide range of their values. The dependences of the pulse reactions maximum values over-the-horizon channels of the OECS on the variations of these parameters are established.

Keywords: atmosphere, scattered laser radiation, bistatic (over-horizon) optical communication, limit base distances, limit pulse transmission frequency

1. INTRODUCTION

Wireless optical communication through atmospheric channels develops in two directions: within the line of sight of the source by the receiver

and outside it. The main advantage of the first type of communication is a high-speed data transmission. Disadvantages are interruption or impossibility of data transmission, associated with obstacles to the propagation of information signals and “running of the beam” on the input pupil of the receiver optical system, due to the turbulent pulsations of optical characteristics in the atmospheric communication channel. These disadvantages are deprived of optical communication out of the sight line, which allows it to be carried out at much greater distances.

In the foreign literature opto-electronic communication systems (OECS) are called “Non Line-of-Sight” (“NLOS”), and in the Russian literature they are called “over the horizon or bistatic OECS”. There are much less works on these systems in the Russian and foreign press, than about the systems used within the line of sight. As it follows from [1–7], the over-horizon OECS can be divided into multicast optical communications at short and at long distances.

The first results of studies of some OECS bistatic channels characteristics are published in the article [5]. The studies were fulfilled in the Zuev Atmospheric optics Institute (AOI) of the Siberian branch of the Russian Academy of Sciences (SbRAS). The subsequent field experimental studies results of the transfer properties of these channels are considered in articles [6–8]. In particular in [8], it is reported that in the experiments the over-horizon communication at cloudless atmosphere at distances up to 70

km between the source of laser radiation with the wavelength $\lambda = 510.6$ nm and the receiver of radiation was realised. We have supplemented the experimental studies by the theoretical studies in order to predict the effect of a particular optical state of the atmosphere on the quality of communication and determine the optimal geometric scheme of its implementation.

The main results of our previous theoretical studies were published in articles [5, 9, 10]. The simulation of the response of the atmosphere as a linear system on the input of the Delta-pulse (i.e., the determination of the impulse response or the impulse response characteristics $h(t)$) and search (using this function) of the optimal communication patterns were their goal. In the framework of this problem in [9] the algorithm of the modified double local estimation of the Monte Carlo method of the nonstationary radiation transfer equation solution is proposed and considered [11]. The proposed algorithm makes a double local estimate at each point of collision in each possible time interval. The proposed algorithm [9] was taken as a basis in this work. In articles [9, 10] this algorithm is compared with the algorithms of statistical modelling of the function $h(t)$, proposed by other authors [12, 13]. Using the proposed algorithm, we have: 1) the analysis of ambient communication channels-scattered laser radiation, when the axis of the laser beam and the optical axis of the receiver lie in the same plane perpendicular to the earth's surface (flat model of the system atmosphere-land surface) and zenith angles of these axes are 85° ; 2) the maximum communication range and the maximum of information transmission speed at $\lambda = 0.5 \mu\text{m}$ and the characteristics of the receiving and transmitting system; 3) the comparison of transmission properties of channels on the wavelength $\lambda = 0.3, 0.5$ and $0.9 \mu\text{m}$ [14].

We considered here the general case, when restrictions on the position in space of the plane containing the axes of the laser beam and the receiving optical system, and on the zenith angles values of these axes orientation are removed.

2. THE PROBLEM STATEMENT

Knowing the response of the atmosphere (as a linear system) to the input Delta-pulse (impulse response) and the input signal, we can determine the received signal as a convolution integral of the form:

$$P(t) = S \int_0^\infty P_0(t')h(t-t')dt' = S \cdot p(t),$$

where S is the photodetector's receiving aperture area; $p(t)$ is the received radiation power, referred to the unit of the receiving aperture area; $P_0(t)$ is the power time function of the radiation source.

The atmospheric channel action of the OECS is considered as the action of a linear system (assuming the absence of nonlinear effects in the interaction of radiation with the medium in the communication channel). The definition of the impulse response of the atmospheric channel of OECS is performed as follows. We consider a plane system "atmosphere-Earth surface" without taking into account reflections from the earth's surface. The atmosphere is an aerosol-gas medium, which has the thickness about 100 km and is divided into 32 homogeneous layers, for every of which we use the optical parameters of the aerosol-gas atmosphere. The upper boundary of the first layer is set at an altitude of 0.1 km from the Earth surface, upper boundary of the second layer is set at an altitude of 0.5 km, and the boundaries of the layers from the third to the twenty third one have a step of 1 km. For subsequent layers, their thickness gradually increases from 2 to 30 km (the values of layer thickness are not given more detailed in this article, since they have little influence on the results of our calculations).

The geometric formation scheme of the communication channel is shown in Fig. 1. At the beginning of the coordinates on the Earth surface there

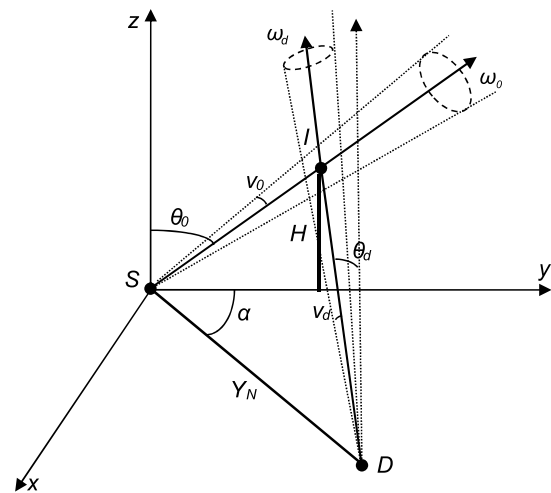


Fig. 1 Geometric scheme of atmospheric bistatic communication line

Table 1. Optical Parameters of the Near Ground Surface (0–0.1 km) Layer of the Atmosphere Used in the Calculations ($\sigma_{t,a}$ is aerosol attenuation coefficient, $\sigma_{s,a}$ is Aerosol Scattering Coefficient, $\sigma_{t,m}$ is Molecular Attenuation Coefficient, $\sigma_{s,m}$ is molecular Scattering Coefficient)

$\lambda, \mu\text{m}$	S_M, km	$\sigma_{t,a}, \text{km}^{-1}$	$\sigma_{s,a}, \text{km}^{-1}$	$\sigma_{t,m}, \text{km}^{-1}$	$\sigma_{s,m}, \text{km}^{-1}$
0.3	10	0.661	0.620	0.165	0.140
0.3	50	0.113	0.106	0.165	0.140
0.5	10	0.433	0.410	0.0166	0.0165
0.5	50	0.0739	0.0700	0.0166	0.0165
0.9	10	0.215	0.196	0.137	0.0015
0.9	50	0.0367	0.0334	0.137	0.0015

is a point source of radiation with the coordinates (0,0,0) with the beam divergence ν_0 oriented in the direction ω_0 in the plane Syz at a zenith angle θ_0 . At the base distance Y_N at an angle α from the Syz plane on the Earth surface there is the receiving system, which has the optical axis oriented to the point I on the axis of the source beam located at a height H from the Earth surface. The zenith angle of the receiving system optical axis is θ_d , and the angle of its field of view is ν_d .

Let it be required to determine the pulse reaction of the OECS bistatic channel for the given conditions of its formation. The plane Syz is called the source plane, and the plane SID is called the plane of the receiver.

3. CALCULATION RESULTS

The program calculations based on the algorithm of the modified double local estimation [9] were performed under the following optical-geometric conditions: radiation wavelengths $\lambda = 0.3, 0.5, \text{ and } 0.9 \mu\text{m}$; meteorological visibility ranges $S_M = 10 \text{ and } 50 \text{ km}$. The generator of optical models sets optical parameters of cloudless aerosol-gas atmosphere at the specified S_M on the basis of the program “LOWTRAN7” [15]. The values of optical factors for the above ground layer of the atmosphere are given in Table 1. At the same time $\theta_0 = 0^\circ, 45^\circ, \text{ and } 85^\circ$; $\nu_0 = 0.0034^\circ$; $Y_N = 0.5\text{--}50 \text{ km}$; $\alpha = 0^\circ, 10^\circ, 30^\circ, 60^\circ, \text{ and } 90^\circ$; $H = H_{min} = 0.1, 0.5, 1, 3, \text{ and } 5 \text{ km}$; $\nu_d = 2^\circ$; the maximum trajectory length $l_{max} = 200 \text{ km}$ (without Y_N). The H_{min} was taken as the height, at which $\theta_d = 85^\circ$. The total calculations were performed for 2412 variants of optical-geometric conditions. The calculation of one variant depended on the conditions of calculations and was about 40 minutes per computer with the performance 19.5 GFlops on the LIN-X test.

The average time interval error of the obtained results of calculations for $S_M = 50 \text{ km}$ was 0.1–6.2 % in all considered variants, and for $S_M = 10 \text{ km}$ it was 0.1–9 % with the exception of the variants with $\lambda = 0.3 \text{ and } 0.5 \mu\text{m}$ for $Y_N \geq 30 \text{ km}$, in which the average time interval error lies within 0.16–34 %. Illustrations of some calculation results of the impulses maxima, which response for time intervals h_{max} when $H = H_{min}$ are shown in Fig. 2.

The dependence analysis of the h_{max} on optical-geometric conditions shows that for small base distances Y_N (2–3 km), other things being equal, h_{max} is maximal for $\lambda = 0.3 \mu\text{m}$. At large Y_N and at low atmospheric turbidity ($S_M = 50 \text{ km}$), h_{max} is maximal for $\lambda = 0.5 \mu\text{m}$. At high atmospheric turbidity ($S_M = 10 \text{ km}$), the behaviour of h_{max} is more complex. At small α (near 0°) at $Y_N = 2\text{--}10 \text{ km}$, h_{max} is maximal for $\lambda = 0.5 \mu\text{m}$, and at $Y_N > 10 \text{ km}$, h_{max} is maximal for $\lambda = 0.9 \mu\text{m}$ (Fig. 2, (a)). However, at $\alpha \geq 10^\circ$ and $Y_N > 2 \text{ km}$, h_{max} is maximal for $\lambda = 0.5 \mu\text{m}$.

The reason for such dependence of the h_{max} values on the variable parameters is that at $\lambda = 0.3 \mu\text{m}$ not only the radiation scattering is stronger, but also its attenuation (due to ozone absorption) is greater than at other λ ; this greatly reduces the received signal power at large Y_N . The role of scattering and attenuation at $\lambda = 0.5$ is higher than at $\lambda = 0.9 \mu\text{m}$ at high atmospheric turbidity and lower absorption (due to the presence of water vapour absorption at $\lambda = 0.9 \mu\text{m}$).

The calculations also show that, other things being equal, h_{max} at $H = H_{min}$ is higher than at any $H > H_{min}$. This is due to the fact that when $H = H_{min}$ the length of the path SID and the scattering angles of the trajectories are minimal on the average.

Knowing the characteristics of the receiving and transmitting equipment and the pulse response of the atmospheric channel, it is possible to determine

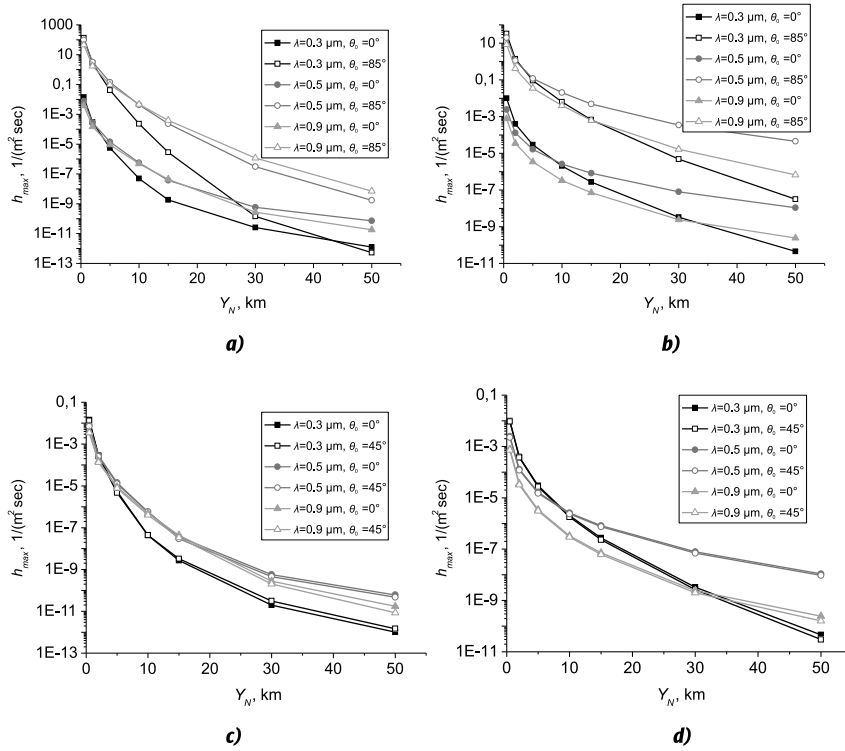


Fig. 2. Maximum impulse response $h_{max}(Y_N)$ at:
 $S_M = 10 \text{ km}, \alpha = 0^\circ, \theta_d = 85^\circ$ (a);
 $S_M = 10 \text{ km}, \alpha = 60^\circ, \theta_d = 85^\circ$ (c);
 $S_M = 50 \text{ km}, \alpha = 0^\circ, \theta_d = 85^\circ$ (b);
 $S_M = 50 \text{ km}, \alpha = 60^\circ, \theta_d = 85^\circ$ (d)

the limit range of the communication line. As an appropriate example, we consider a laser with $\lambda = 0.5 \mu\text{m}$ as a transmitting information system. Suppose that the laser pulse shape is rectangular, its duration $\Delta t = 30 \text{ nsec}$ and the average pulse power $P_0 = 18182 \text{ W}$. Let the amplifier element (PMT-17A) used as a part of an ideal receiving optical system. For the maximum range of communication for given α and θ_0 , we take Y_N , in which the power level of the received radiation P matches the limit. For the upper bound of P we take the maximum P used under the given conditions.

With the growth of Y_N , the values of the impulse response are changed many times, so it makes sense to consider the value of the ratio P_0 to P reduced to decibels, η [2]:

$$\eta = 10 \lg(P_0/P) = 10 \lg\left(\frac{P_0}{pS}\right),$$

where p is the power of the received radiation per unit area of the aperture, S is the area of the aperture.

Then the limit Y_N will be the distance, at which

$$\eta > \eta_*, \eta_* = 10 \lg\left(\frac{P_0}{P_*}\right),$$

where P_* is the limit of P_0 .

As a limit, we take the power that satisfies the ratio [16–18]

$$\rho = \frac{F \Sigma_A M}{\sqrt{2e \Delta f [M^2 I_k (1+B) + \frac{2kT}{e R_i} (1 + \frac{R_e}{R_i})]}} = 1, \quad (1)$$

where

$$M = \frac{\Sigma_A}{\Sigma_c}, \Delta f = \frac{1}{2R_i C_a}, \quad (2)$$

$$I_k = \Sigma_c \cdot F + I_k + \Sigma_c \cdot F_b, I_k = j_T \cdot Q,$$

ρ is the signal-to-noise ratio; I_k is the mean value of the photocathode emission current; F is an average value of the luminous flux measured; Σ_c is the photocathode integral sensitivity; Σ_A is the anode sensitivity; R_e is the equivalent noise resistance; $(1+B)$ is the noise factor; T is the absolute temperature of the photomultiplier (PMT); M is the gain of the PMT; Δf is the frequency band; R_i is the load resistance; C_a is the capacitance between the anode output and the last cascade; F_b is the background illumination; I_{tk} is the current of the photocathode thermal emission; j_T is the thermoelectric current density; Q is the photocathode area.

Table 2. Constants of Approximation for the Calculation of η

$\lambda, \mu\text{m}$	S_M, km	C_1, dB	C_2, dB	$C_3, \text{dB/rad}$	N_0	C_4	C_5
0.5	10	114	-33.4	35.2	0.109	0.024	-0.016
0.5	50	120	-31.2	31.8	0.076	0.007	-0.003

The following values were used in the calculations (1) and (2) [6, 16–21]: $\Sigma_c = 40 \mu\text{A/lm}$ [20, P. 134]; $\Sigma_A = 10 \text{ A/lm}$ [20, P. 134]; $R_l = 10^8 \text{ Ohm}$ [18, P. 274]; $C_a = 10^{-11} \text{ F}$ [18, P. 274]; $1 + B = 2.5$ [18, P. 274]; $T = 256 \text{ K}$ [6]; $R_e = 3.5 \cdot 10^6 \text{ Ohm}$ [20, P. 161]; $j_T = 10^{-15} \text{ A/cm}^2$ [16, P. 109]; $Q = 0.8 \text{ cm}^2$ [19, P. 46]; $F_b = 0 \text{ lm}$.

Our earlier estimates [14] for the PMT-17A showed that $F = 2 \cdot 10^{-11} \text{ lm}$ in the conditions considered by us. For conversion from lm to W we have the equation

$$P = \frac{F}{Cv(\lambda)},$$

where $C = 683 \text{ lm/W}$; $v(\lambda) = 0.323$ at $\lambda = 0.5 \mu\text{m}$ [21, P. 23].

In this article, we consider a special case when $F_b = 0 \text{ lm}$. The case of the presence of a solar background will be the subject of the following works. The algorithm of statistical modelling of the background radiation is developed and tested by us in the framework of [22].

For the maximum P and for cases, when $H = H_{min}$ (that corresponds to the best conditions for P), the ratio η was calculated. An approximation of its form was constructed for its description

$$\eta(\theta_0, Y_N, \alpha) =$$

$$= \left(C_1 + C_2(1 - \cos \theta_0) + C_3|\alpha|(1 - \cos \theta_0) \right) \left(\frac{Y_N}{0.5} \right)^{N_0 + C_4\theta_0 + C_5\theta_0|\alpha|}, \quad (3)$$

where $C_1 - C_5, N_0$ are the approximation constants.

The applicability conditions of the formula (3) are: $\theta_d = 85^\circ$ ($H = H_{min}$), $-90^\circ < \alpha < 90^\circ$, $0^\circ < \theta_0 < 85^\circ$, and $Y_N = 0.5 - 50 \text{ km}$. The values of the approximation constants are given in Table 2. The absolute approximation error at $S_M = 50 \text{ km}$ is 0.01–9.06 dB; the absolute approximation error at $S_M = 10 \text{ km}$ is 0.02–12.8 dB.

Using the approximation (3), the dependences η on the location of the receiving system and θ_0 for the situations, when $\eta < 173 \text{ dB}$ are constructed (Fig. 3). The figure shows that the obtained dependences are in full agreement with the conclusions obtained for the h_{max} dependencies.

Another factor that characterizes the quality of the communication channel is the limit number of pulses per unit of time, which can be transmitted and received through the communication channel. This characteristic is related to the speed of information transmission. Following the work [2], as the

Table 3. The Range of Variation of v_{max}

$\theta_0, ^\circ$	$\alpha, ^\circ$	$v_{max}(0.5)$	$v_{max}(50)$	$\theta_0, ^\circ$	$\alpha, ^\circ$	$v_{max}(0.5)$	$v_{max}(50)$
$S_M = 10 \text{ km}$				$S_M = 50 \text{ km}$			
0		4.53E+06	7.65E+03	0		4.61E+06	3.29E+04
45	0	1.04E+07	1.71E+04	45	0	1.05E+07	8.58E+04
45	10	1.03E+07	1.82E+04	45	10	1.03E+07	8.34E+04
45	30	9.06E+06	1.28E+04	45	30	9.15E+06	6.88E+04
45	60	6.45E+06	8.48E+03	45	60	6.55E+06	4.34E+04
45	90	4.34E+06	6.15E+03	45	90	4.44E+06	2.77E+04
85	0	1.99E+07	7.22E+04	85	0	1.99E+07	1.09E+06
85	10	1.87E+07	2.14E+04	85	10	1.88E+07	3.88E+05
85	30	1.22E+07	9.15E+03	85	30	1.24E+07	4.95E+04
85	60	2.72E+06	4.43E+03	85	60	2.89E+06	1.07E+04
$v_{max}(A) = v_{max}(A = Y_N)$							

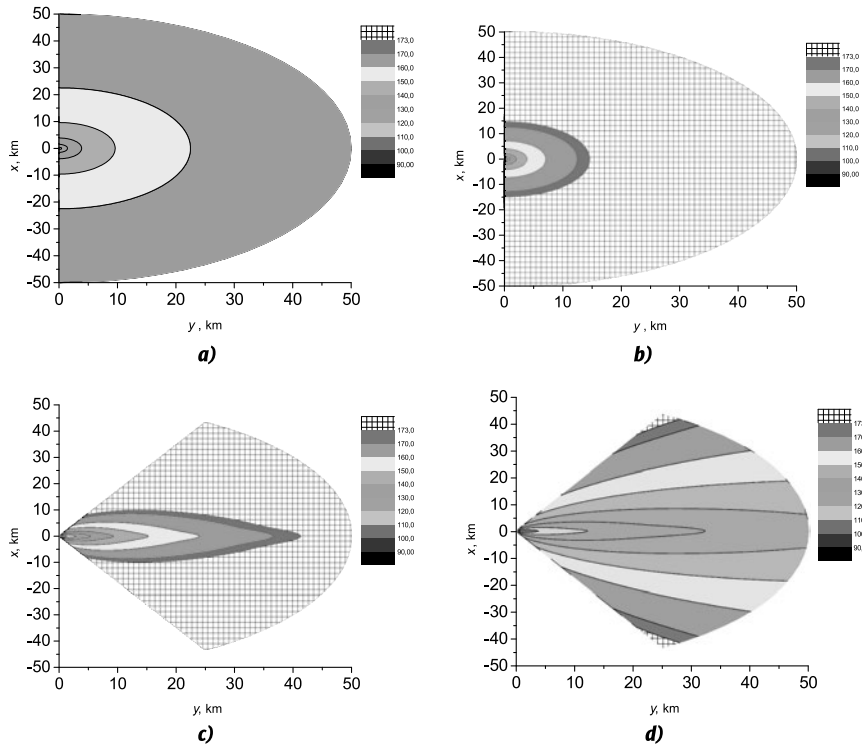


Fig. 3. Dependence $\eta(x, y)$ at $\lambda = 0.5 \mu\text{m}$ at:
 $S_M = 50 \text{ km}, \theta_0 = 0^\circ$ (a);
 $S_M = 10 \text{ km}, \theta_0 = 0^\circ$ (b);
 $S_M = 50 \text{ km}, \theta_0 = 85^\circ$ (c);
 $S_M = 10 \text{ km}, \theta_0 = 85^\circ$ (d)

pulses transmission limit frequency ν , which allows the communication channel, we can take the value of ν_{max} defined implicitly as:

$$\frac{|F[P(t)](\nu_{max})|}{|F[P(t)](0)|} = 0.5,$$

$$F[P(t)](\nu) = \int_{-\infty}^{+\infty} P(t)e^{2\pi i\nu t} dt,$$

where $P(t)$ is the power distribution of the received radiation; F is the Fourier transform.

ν_{max} values were calculated for the optical-geometrical conditions and characteristics of the receiving-transmitting equipment described above. Examples of calculation results are shown in Fig. 4, and Table 3 shows the range of ν_{max} changes in the Y_N from 0.5 to 50 km and different values of θ_0 and α . The calculation results show that ν_{max} decreases with the growth of Y_N and α . At small Y_N (up to 5 km) ν_{max} weakly depends on the turbidity of the medium, and at large Y_N with increasing turbidity ν_{max} decreases several times. From Table 3 it follows that ν_{max} lies in the range from $4 \cdot 10^3$ to $2 \cdot 10^7$ Hz at $\Delta t = 30$ nsec and at the specified parameters of the transmitting-receiving communication system.

4. CONCLUSION

The simulation program by the Monte Carlo method of bistatic atmospheric aerosol-gas channels pulse reactions of OECS is created on the basis of the modified double local estimation algorithm [9, 10]. This program is used in a series of numerical experiments to statistically evaluate the transfer characteristics of these channels depending on the optical characteristics of an atmosphere plane-parallel model at $\lambda = 0.3, 0.5,$ and $0.9 \mu\text{m}$ at a meteorological visibility range $S_M = 10$ and 50 km. The results are obtained for a set of basic distances (up to 50 km) between the radiation source and the radiation receiver and for the angular orientations of the optical axes of a laser radiation beam and of the receiving system in a wide range of their values. The dependences of the pulse reactions maximum values over-the-horizon channels of the OECS on the variations of these parameters are established.

The upper estimation of the limiting frequencies and the action ranges of the model optical-electronic communication system, which simulates the system already used in field experimental studies, is carried out [7, 8].

The main conclusions from the analysis of the results are as follows: 1) the maximum power of the received information pulse is maximum at $\lambda = 0.3$

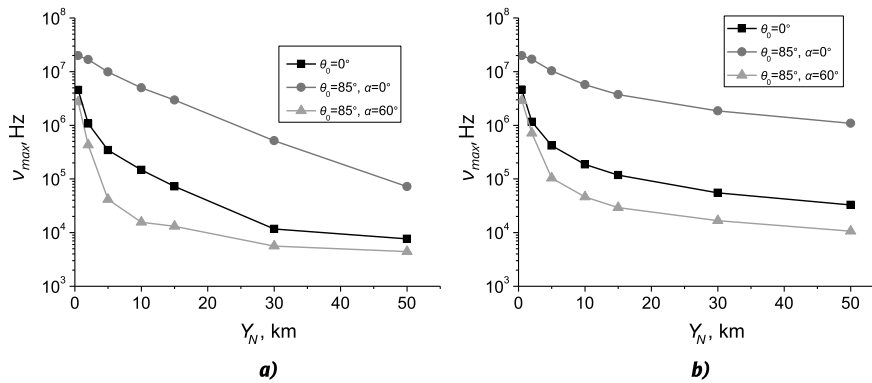


Fig. 4. Dependence of $v_{max}(Y_N)$ at $S_M=10$ km (a) and 50 km (b)

μm at small base distances (2–3 km), other things being equal; 2) the maximum power of the received information pulse can be achieved for $\lambda = 0.5 \mu\text{m}$ at large base distances ($S_M = 50$ km) and low turbidity; 3) it can be achieved for $\lambda = 0.5$ and $0.9 \mu\text{m}$ at high turbidity of the atmosphere ($S_M = 10$ km) depending on the basic distances and the orientation of the reception plane.

The limiting pulse transmission frequencies for bistatic communication optoelectronic systems depending on the optical state of the atmosphere and the geometrical parameters of the communication channel formation schemes lie in the range from $4 \cdot 10^3$ to $2 \cdot 10^7$ Hz.

The work was performed with financial support within the Priority direction II.10, project II.10.3.3. “Direct and inverse problems of sounding of the atmosphere and the Earth surface, atmospheric correction, and communication by optical-electronic systems using scattered laser radiation”.

REFERENCES

1. Poller B.V., Britvin V.A., Kolomnikov J.D., Golovachev Yu.G., Konyaev S.I., Kusakina A.E., Shergunova N.A. Nekotory'e xarakteristiki rasprostraneniya lazerny'x signalov v usloviyax observatorii SO RAN “Kajtanak” na gornom Altae [Some of the characteristics of laser signals propagation in Observatory of the Russian Academy of Sciences of “Kaytanak” in mountain Altai] // Interexpo geo-Siberia, 2012, Vol. 2, #4, pp. 64–68.
2. Haipeng D., Chen G., Arun K., Sadler B.M., Xu Z. Modeling of non-line-of-sight ultraviolet scattering channels for communication // IEEE journal on selected areas in communications, 2009, Vol. 27, #9, pp. 1535–1544.
3. Han D., Liu Y., Zhang K., Luo P., Zhang M. Theoretical and experimental research on diversity reception technology in NLOS UV communication system // Optics express, 2012, Vol. 20, #14, pp. 15833–15842.
4. Elshimy M.A., Hranilovic S. Non-line-of-sight single-scatter propagation model for noncoplanar geometries // JOSAA, 2011, Vol. 28, #3, pp. 420–428.
5. Borisov B.D., Belov V.V. Vliyanie pogodny'x uslovij na parametry' korotkogo lazernogo impul'sa, otrazhyonnogo atmosferoj [Influence of weather conditions on the parameters of short laser pulses reflected from the atmosphere] // Optika atmosfery' i okeana, 2011, Vol. 24, #4, pp. 263–268.
6. Belov V.V., Tarasenkov M.V., Abramochkin V.N., Ivanov V.V., Fedosov A.V., Troitskiy V.A., Shiyanyan D.V. Atmosferny'e bistaticheskie kanaly' svyazi s rasseyaniem. Chast' 1. Metody' issledovaniya [Atmospheric bistatic communication channels with scattering. Part 1. Research methods] // Optika atmosfery' i okeana, 2013, Vol. 26, № 4, pp. 261–267.
7. Belov V.V., Tarasenkov M.V., Abramochkin V.N. Bistaticheskie atmosferny'e optiko-e'lektronny'e sistemy' svyazi (polevy'e e'ksperimenty') [Bistatic atmospheric optoelectronic communication systems (field experiments)] // Pis'ma v ZhTF, 2014, Vol. 40, #19, pp. 89–95.
8. Abramochkin V.N., Belov V.V., Gridnev Yu.V., Kudryavtsev A.N., Tarasenkov M.V., Fedosov A.V. Optiko-e'lektronnaya svyaz' v atmosfere na rasseyannom lazernom izluchenii. Polevy'e e'ksperimenty' [Optical-electronic communication in the atmosphere on scattered laser radiation. Field experiments] // Svetotekhnika, 2017, #4, pp. 24–30.
9. Belov V.V., Tarasenkov M.V. Tri algoritma statisticheskogo modelirovaniya v zadachax opticheskoy svyazi na rasseyannom izluchenii i bistaticheskogo zondirovaniya [Three algorithms of statistical simulation in tasks of optical communication for scattered radiation and bistatic sounding] // Optika atmosfery' i okeana, 2016, Vol. 29, #5, pp. 397–403.

10. Tarasenkov M.V., Belov V.V. Sravnenie trudoyomkosti algoritmov statisticheskogo modelirovaniya impul'snoj reakcii kanala bistaticheskoy lazernoj svyazi na rasseyannom izlucheni i bistaticheskogo lazernogo zondirovaniya [Comparison of complexity of algorithms of statistical simulation of the impulse response of the channel bistatic laser communication for scattered radiation and bistatic laser sounding] // Vy'chislitel'ny'e tekhnologii, 2017, Vol. 22, #3, pp. 91–102.

11. Marchuk G.I., Mikhailov G.A., Nazaraliev M.A., Darbinyan, R.A., Kargin B.A., Elepov B.S. Metod Monte-Karlo v atmosfernoj optike [Monte-Carlo in atmospheric optics] // Nauka, Siberian branch, Novosibirsk, 1976, 284 p.

12. Lotova G.Z. Modification of the double local estimate of the Monte Carlo method in radiation transfer theory // Russian Journal of Numerical Analysis and Mathematical Modeling, 2011, Vol. 26, #5, pp. 491–500.

13. Mikhailov G.A., Lotova G.Z. Chislenno-statisticheskaya ocenka potoka chasticz s konechnoj dispersiej [Numerical and statistical estimation of the particle flow with finite dispersion] // DAN, 2012, Vol. 447, #1, pp. 18–21.

14. Tarasenkov M.V., Belov V.V., Poznakhareva E.S. Modelirovanie processa peredachi informacii po atmosfery'm kanalam rasprostraneniya rasseyannogo lazernogo izlucheniya [Modeling of the process of information transfer in the atmospheric distribution of scattered laser radiation] // Optika atmosfery' i okeana, 2017, Vol. 30, #5, pp. 371–376.

15. Kneizys F.X., Shettle E.P., Anderson G.P., Abreu L.W., Chetwynd J.H., Selby J.E.A., Clough S.A., Gallery W.O. User Guide to LOWTRAN-7. ARGL-TR-86-0177. ERP 1010. Hansom AFB. MA 01731, 1988, 137 p.

16. Anisimov I.I., Glukhovskij, B.M. Fotoe'lektronny'e umnozhiteli [Photomultipliers] // Sov. Radio, Moscow, 1974, 61 p.

17. Aksenenko M.D., Baranochnikov M.L. Priyomniki opticheskogo izlucheniya: spravochnik [Optical radiation Receivers: Handbook] // Radio i svyaz', Moscow, 1987, 296 p.

18. Soboleva N.A. Melamid, A.E. Fotoe'lektronny'e pribory' [Photoelectronic devices] // Vy'ssh. shkola, Moscow, 1974, 376 p.

19. Vasiliev A.F., A.M. Chmutin. Fotoe'lektricheskie priyomniki izlucheniya [Photoelectric radiation detectors] // VolGU, Volgograd, Russia, 2010, 81 p.

20. Chechik N.O., Feinstein S.M., Lifshitz T.M. E'lektronny'e umnozhiteli. Pod red. D.V. Zernova [Electronic multipliers. Edited by D.V. Zernov] // GITTL, Moscow, 1957, 576 p.

21. Gurevich M.M. Fotometriya (teoriya, metody' i pribory') [Photometry (theory, methods and devices)] // Energoatomizdat, Leningrad, USSR, 1983, 272 p.

22. Belov V.V., Tarasenkov M.V., Piskunov K.P. Parametricheskaya model' solnechnoj dy'mki v vidimoj i UF-oblasti spectra [Parametric model of solar haze in the visible and UV region of the spectrum] // Optika atmosfery' i okeana, 2010, Vol. 23, #4, pp. 294–297.



Mikhail V. Tarasenkov, Ph.D. in Phys. and Math. Science. He graduated from the Tomsk State University (TSU) in 2007. Senior researcher at the Zuev Institute of atmospheric optics.

Research interests: analysis of regularities of image formation through the atmosphere, atmospheric correction of images in the visible and UV radiation ranges, theoretical research on communication channels outside the line of sight



Egor S. Poznakharev, student of the TSU. Engineer of the Zuev Institute of atmospheric optics. Research interests: theoretical and experimental research on communication channels outside the line of sight



Vladimir V. Belov, Dr. of Phys. and Math. Science, Prof. He graduated from the TSU in 1971. Head of ROS laboratory of the Zuev Institute of atmospheric optics.

Honored worker of science of Russia. Research interests: theory of optical radiation transfer in scattering and absorbing media, theory of laser sensing, theory of vision, atmospheric correction of aerospace images of the Earth surface, Monte Carlo method, multiple scattering